

Published in final edited form as:

Acta Biomater. 2013 January ; 9(1): 4935–4943. doi:10.1016/j.actbio.2012.09.003.

Enhanced Cellular Adhesion on Titanium by Silk Functionalized with titanium binding and RGD peptides

Guillaume Vidal^a, Thomas Blanchi^b, Aneta J. Mieszawska^c, Rossella Calabrese^c, Claire Rossi^d, Pascale Vigneron^a, Jean-Luc Duval^a, David L. Kaplan^c, and Christophe Egles^{a,e,*}

^aUMR CNRS 7338 - Biomécanique et BioIngénierie, Centre de Recherches de Royallieu 60205 Compiègne Cedex France

^bDepartment Of Periodontology, Tufts University, School of Dental Medicine, 1 Kneeland Street, Boston MA 02111 USA

^cBiomedical engineering, Science & Technology Center, 4 Colby Street, Tufts University, Medford, MA 02155 USA

^dUMR CNRS 6022 - Génie Enzymatique et Cellulaire, Centre de Recherches de Royallieu 60205 Compiègne Cedex France

^eDepartment of Oral and Maxillofacial Pathology, Tufts University, School of Dental Medicine, 1 Kneeland Street, Boston MA 02111 USA

Abstract

Soft tissue adhesion on titanium represents a challenge for implantable materials. In order to improve adhesion at the cell/material interface we used a new approach based on the molecular recognition of titanium by specific peptides. Silk fibroin protein was chemically grafted with titanium binding peptide (TiBP) to increase adsorption of these chimeric proteins to the metal surface. Quartz Crystal Microbalance was used to quantify the specific adsorption of TiBP-functionalized silk and an increase in protein deposition by more than 35% was demonstrated due to the presence of the binding peptide. A silk protein grafted with TiBP and fibronectin-derived RGD peptide was then prepared. The adherence of fibroblasts on the titanium surface modified with the multifunctional silk coating demonstrated an increase in the number of adhering cells by 60%. The improved adhesion was demonstrated by Scanning Electron Microscopy and immunocytochemical staining of focal contact points. Chick embryo organotypic culture also revealed strong adhesion of endothelial cells expanding on the multifunctional silk-peptide coating. These results demonstrated that silk functionalized with TiBP and RGD represents a promising approach to modify cell-biomaterial interfaces, opening new perspectives for implantable medical devices, especially when reendothelialization is required.

Keywords

silk protein; titanium-binding peptide; peptide grafting; cell adhesion; surface modification

© 2012 Acta Materialia Inc. Published by Elsevier Ltd. All rights reserved.

*Corresponding author: Christophe Egles, Université de Technologie de Compiègne (France), Bureau G212, Centre de Recherches, BP 20529, Rue Personne de Roberval, 60205 Compiègne - France, Tel.: 33 (0)3 44 23 44 22, christophe.egles@utc.fr.

Publisher's Disclaimer: This is a PDF file of an unedited manuscript that has been accepted for publication. As a service to our customers we are providing this early version of the manuscript. The manuscript will undergo copyediting, typesetting, and review of the resulting proof before it is published in its final citable form. Please note that during the production process errors may be discovered which could affect the content, and all legal disclaimers that apply to the journal pertain.

Introduction

The adhesion of cells or tissues at the surface of implanted materials requires specific surface modifications [1]. Different strategies have been tested that use a physical or chemical modification such as abrasion or acid etching of the metal [2],[3]. More recently, a new approach was developed, using the specific biological activity linked to short peptidic sequences. Since 1984, it has been realized that a large number of glycoproteins of the extracellular matrix including fibronectin, contain the tripeptide arginine-glycine-aspartic acid (RGD) as cell recognition sites [4]. Integrins are highly selective and generally bind to « *GRGDSP* » with high affinity to the $\alpha 5/\beta 1$ integrin [5]. Thus, functionalization of implant surfaces with a specific RGD peptide can selectively direct one type of cell adhesion receptor [6].

Different strategies have been proposed to bind these peptides to metallic implants, especially widely used titanium. It has been suggested that stable linking of the RGD peptide to the surface was essential to promote strong cell adhesion [6],[7]. Indeed, titanium dioxide (TiO_2) is one of the most widely explored bio-related materials, particularly in relation to medical implants. Forming a stable layer on the surface of titanium-based implants provides a highly active oxide that mediates interactions with surrounding proteins, in turn governing the integration of the implants with the surrounding tissues [8],[9]. A number of extracellular matrix proteins (e.g., fibronectin) and plasma proteins (e.g., fibrinogen and albumin) strongly interact with TiO_2 . These interactions are often mediated via weak associations, including ionic forces and hydrogen bonds, resulting in unstable, highly reversible protein adsorption to TiO_2 [10],[11]. However, the adherence of proteins on the surface of metallic materials largely relies on nonspecific hydrophobic interactions, which generally results in the destruction of the protein structure and inactivation of bound biomolecules.

Recently, several groups used combinatorial display technologies to identify amino acids sequences conferring to phages or bacteria the ability to bind to inorganic and synthetic materials [12],[13]. Among these peptides, some demonstrated high affinity for titanium [14],[15]. These peptides provide new opportunities to develop novel interfaces of biomolecules and inorganic materials to increase cell adhesion. Among the different carriers that can be used to support the grafting of titanium binding peptide (TiBP) and RGD peptides, silk-based biomaterials provide a unique platform to study functional material-tissue outcomes. In brief, biomaterials formed from silk fibroin protein provide:

- i. **Biocompatibility and Controlled degradation rate** – The material degrades slowly with minimal negative impact on the surrounding tissues. Silks, used as sutures, are biocompatible and less immunogenic than collagens or polylactic/polyglycolic acids [16],[17],[18].
- ii. **Mechanical and Thermal Integrity** - Native silk fibers exhibit tensile properties and resistance to mechanical compression that exceed all other natural fibers and rival synthetic high performance fibers. Silks can also be autoclaved without any loss of integrity due to their thermal stability [16].
- iii. **Plasticity in Processing and Functionalization** - The hydrophobic nature of silk fibroin provides stability in the shape and size of the fibers under physiological conditions, with available amino acid side chain chemistries for facile chemical functionalization.

The goal of the present study was to functionalize silk fibroin protein with TiBP and RGD peptide to improve cell and soft tissue adhesion on titanium discs. This approach to functionalization of titanium as a way to improve cell interactions could provide a relatively

simple yet very effective strategy to modify the surface chemistry of the implant and lead to the development of completely new strategies in the biomaterial field.

Material and methods

Substrates

Commercially pure titanium discs (CP-Ti, 20-mm diameter, 4-mm thick, surface polished) were kindly provided by Dr. Brigitte Grosogeat (University of Lyon, France) and were thoroughly washed with distilled water, dried and sterilized with 70% ethanol for 30 min before use. All chemicals were purchased from Aldrich, Sigma or Fluka and used as supplied without further purification.

Silk fibroin and subsequent chemical modification

Bombyx mori silkworm cocoons were cut in small pieces and boiled for 1 h in aqueous solution of 0.02 M Na₂CO₃, rinsed once with boiling DI water, three times with cold DI water and dried in air using our previously published procedures [19]. The silk fibroin was solubilized in 9M LiBr solution at 60°C to 20wt%, filtered through 5 µm syringe filter, dialyzed for 1 day against deionized water (membrane MWCO 3,500 g.mol⁻¹; Pierce, Woburn, MA), and for two days against BupHTM MES buffered saline (Pierce) at pH 6.5. The final concentration of silk solution in MES buffer was 6–9 wt%. Silk fibroin was modified with RGD peptide (RGD): H-CSSGRGDSP-OH and the titanium-binding peptide (TiBP): H-CGHTMTHYHAVRTQT-OH (Biomatik USA, LLC Wilmington, DE) at two different concentrations: 1.1% and 6.4%. The carboxyl groups of aspartic and glutamic acid (1.1 mol %) of silk fibroin were used for EDC/NHS catalyzed reaction (NHS: N-Hydroxysuccinimide, EDC: 1-Ethyl-3-[3-dimethylaminopropyl] carbodiimide hydrochloride) with the free amine group of the N-terminus of the peptide. Briefly, 0.25 g of NHS and 0.4 g of EDC per gram of dry silk protein was added to the silk fibroin solution and reacted for 30 min; the unreacted EDC was quenched with 2-mercaptoethanol. Next, the peptides were added at 1:1 molar ratio, with respect to available carboxyl groups, and the reaction was allowed to proceed for 3 h. The addition of NaOH to increase the pH to 9 stopped the coupling reaction. The modified silk fibroin solutions were dialyzed against DI water for 2 days, changing water 3 times a day. The final products were silk fibroin modified with (1) RGD, (2) TiBP, and (3) 50:50 mix of RGD and TiBP. Additionally, the tyrosine residues of silk fibroin were modified using diazonium coupling chemistry as we have described previously [20], to increase the carboxyl group content by 5.3 mol% to a total of 6.4 mol%. The EDC/NHS catalyzed reaction was used as described above to prepare the corresponding silk fibroin/peptide constructs at higher peptide loads.

Amino acid composition analysis

Amino acid composition analysis was performed at the W.M. Keck Foundation Biotechnology Resource Laboratory (Yale University, New Haven, CT). Samples analyzed were Silk-TiBP 5.3%, Silk-RGD 5.3%, and Silk-TiBP/RGD 5.3%, along with the starting unmodified silk (referred to as Silk(Y)-COOH, with carboxyl group content ~ 5.3%). Aliquots of 10 µl of 1mg/ml aqueous solution from each sample were lyophilized and hydrolyzed in vacuum for 16 h at 115°C in 6N HCl/0.2% phenol with 1 nmole/100 µl nVal as an internal standard. Samples (10% of each aliquot) were quantified using a Hitachi L-8900PH Amino Acid Analyzer (Ion-exchange separation followed by post-column derivatization with ninhydrin for detection at 570 nm and 440 nm). Data were analyzed with EZChrom Elite for Hitachi data acquisition software.

Functionalization of titanium discs

2.5% (w/v) silk fibroin solutions were cast onto the titanium discs for one hour at room temperature. The discs were rinsed in PBS for 10 minutes and dried in an oven for one hour at 55°C. The dried discs were treated with 70% methanol for 2 hours to ensure insolubility of the silk in aqueous media and allowed to dry in air under a laminar flow hood overnight. Titanium discs were sterilized with 70% ethanol for 30 min before use.

Quartz Cristal Microbalance with Dissipation measurements

Measurements were performed with the Q-Sense E1 instrument (Q-Sense, Gothenburg, Sweden) as described in [21]. Protein solutions (2 mL, 100µg/mL) were pumped through the sensor chamber by a peristaltic pump at a flow rate of 500µL/min. After the protein injection, the flow was stopped for 4 min, before the buffer rinsing step. The buffer solution was pumped through the sensor cell at 500µL/min during 4 min.

Cell culture

Swiss 3T3 albino fibroblast cells were obtained from the American Type Culture Collection (ref CCL-92) and cultured in Dulbecco's modified Eagle medium with 4 mM L-glutamine (GIBCO 25030), 4500 mg/L D-glucose and 0.11 g/L sodium pyruvate (DMEM, Gibco 21969), supplemented with 10% v/v heat inactivated fetal bovine serum (FBS, Gibco 10270-098) and 100 U/mL penicillin 100 µg/mL streptomycin (Penicillin-Streptomycin, Gibco 15140), in incubator under 10% CO₂/90% air. Confluent cells were detached with 0.25% (w/v) trypsin-EDTA (Gibco, 25200), washed and suspended in serum-free medium and used for the experiments described below. The Swiss 3T3 mouse fibroblasts were used in the cell adhesion assays. Experiments with Titanium discs were carried out in both the absence of serum proteins and the presence of 10% FBS (after 4h). The titanium surfaces were seeded at 2×10⁴ cells/cm² in 1500 µl of serum-free medium for 4 h at 37°C and 10% CO₂, then the serum-free medium was replaced with DMEM containing 10% FBS and cells were grown for 4 days with medium replaced with fresh one after 3 days.

Scanning Electron Microscopy

The cells were rinsed in PBS, fixed in 3% glutaraldehyde in Rembaum buffer (pH 7.4) [22] for 1 hour, dehydrated in a series of graded alcohols, critical-point dried from CO₂ (Polaron Instrument Inc., Nottingham UK), sputter-coated with gold (Polaron) and examined in a Philips ESEM-FEG XL30 Environmental Scanning Electron Microscope.

Immunofluorescence imaging

Cells were fixed 4h post-seeding in 1mL of 4% paraformaldehyde solution in phosphate-buffered saline (PBS) for 10 min at room temperature then rinsed three times with PBS. Samples were permeabilized in 0.5% Triton X-100 in PBS for 5 min at room temperature and rinsed twice with PBS before 1h incubation at RT in 1% bovine serum albumin in PBS to minimize non-specific staining. Primary monoclonal antibody mouse IgG1 anti-vinculin (1:100, Chemicon MAB 3574) was added in PBS/BSA 0.1% (w/v) and incubated at RT for 1 h in the dark. The cells were washed with PBS three times. Cy3-conjugated secondary antibody (cy3 goat anti mouse IgG 115-165-146, Jackson ImmunoResearch), DAPI (1µg/mL, D95-64, Sigma) and Phalloidin-X5-505 (0.16 nmol/mL, FP-AZ0130, Fluoroprobes) were added and incubated at RT in the dark for 1 hour. The samples were then rinsed twice with PBS and observed using a LEICA DMI 6000 microscope. For focal contact points' quantification, more than 80 cells on 9 different areas from three independent experiments of each condition (bare titanium or Silk-TiBP/RGD) have been analyzed and vinculin spots counted in a double blind test. Results were compared using a Mann-Whitney test with $p < 0.001$ (***) .

Cell counts

For cell quantification on figure 3, ImageJ analysis software was used (NIH, <http://rsb.info.nih.gov/ij/>). The raw image was converted to an 8-bit file and then converted to a binary image by setting a threshold. Threshold values were determined empirically giving the most accurate image for a subset of randomly selected photomicrographs. Cell number was calculated in randomly selected 400 μm squares by “analyze particles” in ImageJ. Five samples per condition were analyzed and this procedure was repeated five times (n = 5) and the results were compared using a Mann–Whitney test. Differences were considered as significant when $p < 0.05$ (*).

Organotypic Culture Model

This method is usually used to assess the cytocompatibility of biomaterials as a function of cellular migration, proliferation, and adhesion. Briefly, from chick embryos, aortic tissue was isolated and sectioned in 1 mm² pieces. After longitudinal sectioning, the vessel was opened so that the endothelial side faced upwards. The epithelial side of a chick embryonic aorta is placed in contact with a solid nutrient culture matrix (i.e. gel made of culture medium, serum and agar solidified on the bottom of a culture dish). A titanium disc was placed on the upper-endothelial side of this explant. Since the matrix does not allow cellular adhesion, cells from the explant preferentially grow along the titanium. Typically after 7 days incubation at 37°C, migration was determined by measuring the area covered by the cells on the titanium disc (Neutral Red staining) with imageJ software. Some samples were fixed in 3% glutaraldehyde solution and prepared for SEM. The cells that detached from the sample surface after incubation for 5, 10, 20, 30 and 60 min were harvested and counted. The samples were then placed in (0.25%) trypsin-EDTA for 15 min. For the cell proliferation assessment we measured the cell layer areas on the different materials using a stereomicroscope fitted with a camera and the ImageJ software. After that, the cells were removed from the materials slowly by using an enzymatic digestion (diluted trypsin). The cell number of the different cell layers were counted at each step of the treatment (5mn, 10mn, 20mn, 30mn and 60mn) and the cell proliferation is assessed by calculating the cell density of the cell layer grown around the initial explant (number of cells per mm²) [23],[24].

Results/Discussion

Silk-peptide and diazo-carboxy-silk -peptide derivatives

To improve adsorption of proteins and cells on titanium, silk fibroin was chemically grafted with titanium binding (TiBP) and RGD peptides.

Silk grafted with TiBP and/or fibronectin-derived RGD were synthesized by the covalent conjugation of the carboxyl groups of silk (1.1 mol %) with the N-terminal amino group of the peptides, via EDC/NHS chemistry. In order to increase the level of peptide grafting, the same reaction was subsequently performed from diazo-carboxy-modified silk, a silk derivative with higher carboxyl group content (6.4 mol%). Diazo-carboxy-silk was synthesized, as we have previously reported [20], by modifying the tyrosine side chains of silk via diazonium coupling with the p-aminobenzoic acid diazonium salt. The derivative was characterized by ¹H-NMR and the analyses (not shown) were in agreement with our previous results [20].

Degree of substitution of the silk-peptide derivatives

In order to confirm the degree of substitution with the peptide derivatives of diazo-silk, amino acid composition analysis was performed. The starting protein, the diazo-carboxy-silk fibroin (Figure 1) and the peptide derivatives, Silk-TiBP 5.3%, Silk- RGD 5.3%, and Silk-TiBP/RGD 5.3% were analyzed. The amount of serine and arginine increased in the

derivatives bearing the RGD peptide (Silk-RGD and Silk-TiBP/RGD), while the relative amount of threonine, valine, histidine and arginine increased in the derivatives bearing the Ti-binding peptide (Silk-TiBP and Silk-TiBP/RGD). Table 1 shows the estimated degree of substitution of the Silk-diazo derivatives modified with Ti-BP and RGD, as calculated from the relative increase of the nmoles of threonine, histidine or arginine, in the silk derivatives with TiBP or RGD, based on the amino acid composition analysis. Cysteine and tryptophan were eliminated from the analysis because cysteine is partially destroyed by HCl hydrolysis and it is usually detected as a combination of cysteine (co-eluting with or just after proline) and cystine (elutes after alanine), and tryptophan degrades during the HCl hydrolysis. During the hydrolysis step, glutamine and asparagine are converted to glutamic acid and aspartic acid, respectively. The degree of substitution thus calculated is consistent with the theoretical values, based on a maximum amount of reactive carboxyl groups ~ 5.3 mol %, and the results confirm the chemical conjugation.

Protein adsorption on titanium

To investigate in real time the interaction of unmodified and 1% TiBP-functionalized silk proteins with the titanium (TiO_2) substrate, we used the Quartz Crystal Microbalance with Dissipation (QCM-D) technique. This method measures simultaneously two properties of adsorbed layers onto the sensor surface. It is sensitive to the changes in frequency (Δf) as well as the changes in energy dissipation (ΔD) that occurs when molecules binds to an oscillating quartz crystal sensor. The frequency shift is related to the mass uptake and the dissipation shift is characteristic of the viscoelastic nature of the protein layer formed on top of the substrate. This technique has been used in many studies of macromolecule adsorption at liquid-metal interfaces [25]. The QCM-D curves obtained upon binding of unmodified and 1% TiBP functionalized silk proteins onto a TiO_2 surfaces are shown in Figure 2. Changes in frequency (Δf_n) and energy dissipation (ΔD_n) obtained at the three overtones (n) were measured simultaneously: $n = 3$ (15 MHz), $n = 5$ (25 MHz) and $n = 7$ (35 MHz) were plotted as a function of time. For both sets of frequency curves (panel B), an initial frequency change was observed upon injection of unmodified or 1% TiBP silk proteins (arrow 1). This frequency shift corresponded to the mass change associated with protein binding to the titanium surface.

In order to facilitate the comparison of the frequency shifts measured at the different harmonics, the frequency values were divided by the overtone number ($\Delta f_n/n$). Concerning the set of unmodified silk binding curves, saturation was reached at -36 , -35 and -33 Hz for the normalized frequency data at the third, fifth and seventh harmonics respectively, and at $\sim 5.6 \times 10^{-6}$ for the dissipation values (figure 2, panel A). With reference to the set of 1% TiBP silk protein binding curves, saturation was obtained at -49 , -45 and -42 Hz for the frequency shifts at the third, fifth and seventh overtones, respectively, and at $\sim 8 \times 10^{-6}$ for the dissipation data. These dissipation values were high enough to consider the protein layers viscous and to explain the absence of superposition in the frequency curves at the different harmonics. Indeed the viscoelastic properties of the adsorbed film have an impact on the frequency measurement. Furthermore, due to the high viscosity of absorbed protein films, the recorded frequency shifts cannot be converted to protein mass adsorbed onto the crystal surface. The Sauerbrey equation is not relevant for nonrigid adsorbed films [26].

The buffer rinsing (arrow 2) was performed until the frequency and dissipation values were stable. There was an increase and decrease in Δf and ΔD , respectively, at all harmonics for the unmodified silk adsorbed on TiO_2 , stabilized at -28 Hz ($n=3$), -26 Hz ($n=5$) and -24 Hz ($n=7$) for the frequency values and at $\sim 4.7 \times 10^{-6}$ for the dissipation values. For the 1% TiBP silk protein, negligible protein material was desorbed during the washing step (stabilization at -47 Hz ($n=3$), -44 Hz ($n=5$) and -41 Hz ($n=3$) for the frequencies and at

$\sim 7.5 \times 10^{-6}$ for the dissipation) suggesting a stronger interaction of the functionalized protein with the surface compared to the control of unmodified surface.

In conclusion the QCM-D results showed that functionalization with 1% TiBP increased the affinity of the silk protein for titanium surfaces by 37.6 ± 7.5 % (standard errors obtained from three independent measurements, independent protein solutions and sensors).

We wanted to investigate the specificity of TiBP interaction with other surfaces using the QCM technique and found that the binding affinity of the TiBP was similar for titanium, gold and silica (data not shown). A number of recent studies have implicated electrostatic interactions as an important contributor in the adhesion of peptides to such varied substrates as SiO₂, gold, aluminum, titanium and titanium oxide [13],[27]. Sano *et al* [28] suggest that the epitope, or set of molecules recognized by Titanium binding peptide-1 (TBP-1), reflects a local electrochemical geometry on the oxide surface that is shared among Ti, Ag, and Si. Chen *et al* [27] have shown that a dominant peptide sequence (STB1) emerged with cross binding affinity to SiO₂ and TiO₂, and is enriched with basic amino acid residues. Also, the structural flexibility of a linear metal oxides-binding peptide enables it to explore a wider range of conformations to maximize its interaction with TiO₂ and SiO₂ [29].

Therefore, surface functionalization with these peptides could be of particular interest for glass-derived biomaterials especially to increase the bioactivity of scaffolds used in bone reconstruction [30]

Cellular spreading and adhesion

Cellular adhesion was evaluated using mouse Swiss 3T3 fibroblasts proteins on titanium and titanium functionalized with TiBP and RGD-grafted silk. Using a computer-assisted cell counting program, it was determined that after 48h of culture the total number of cells per mm² was increased by 60% when titanium was coated with the TiBP and RGD-grafted silk as compared to the control bare titanium (Figure 3). The cell counting data prompted us to perform morphological analysis until 96h of culture of the different samples, non-coated or coated with Silk-TiBP/RGD. After 48h (Figure 4, titanium 48h) few cells were observed leaving the irregular surface of the sample visible (especially circular crevices resulting from the polishing). Some cell debris was found on the surface and higher magnification images of the non-coated surface (titanium 48h) confirmed the presence of the cellular debris (arrow). Nevertheless, few intact cells could be detected and some extracellular matrix deposits were observed.

In contrast, the Silk-TiBP/RGD coated surface (Silk-TiBP/RGD5.3%, 48h) was covered with cells, with a higher density at the center of the sample. At higher magnification, (Silk-TiBP/RGD5.3%, 48h) these cells are well spread and present many pseudopods helping to anchor the cells to the surface for adhesion. Some traces of extracellular matrix proteins could be seen on the titanium. After 96h, (titanium 96h) the material was scattered with cell and extracellular matrix debris (arrow). At higher magnification a few cells were observed spread on the titanium. A completely different situation appeared was observed when the titanium was coated (Silk-TiBP/RGD5.3%, 96h) where a dense and compact cellular layer covered the surface. At higher magnification these cells appear spread. The fibroblasts appeared elongated, adhering with many pseudopods to the surface as well as between themselves. Because the surface was hardly visible, we could not assess the presence of extracellular matrix proteins on the titanium surface.

To further define potential modifications in the cell-material interactions, immunostaining of proteins involved in early cell adhesion were performed 4h after seeding. Especially we labeled the vinculin, an actin filament (F-actin) binding protein involved in cell-matrix

adhesion [31]. In all the experiments, cells presented a flat morphology and appeared intimately adherent to the surface. However, fibroblasts cultured on Silk-TiBP/RGD were spread and mainly spindle-shaped and elongated with no clear orientation (Figure 5B and D). Cells on bare titanium had a less-defined morphology than cells on the silk which showed strong expression of vinculin (arrows) in the peripheral area and had more typical cell morphology as seen by the strong actin architecture and stress fibers. Decreased expression of vinculin and cytoplasmic localization, lack of focal contact points and weaker continuity of F-actin were observed on bare titanium controls (Figure 5A and C). Quantification analysis confirm that focal contact points occur almost exclusively on Silk-TiBP/RGD functionalized titanium with an average density of 3 spots per cell 4h after seeding (figure 5E).

Cell adhesion and spreading assays showed that TiBP increased the immobilization of the RGD grafted-silk fibroin on the titanium surface while preserving functionality as a recognition site for cells. Next to proper peptide immobilization on the different materials, the design of the RGD peptide itself, as well as its density and arrangement on surfaces, contribute to successful cell attachment. The GRGDS peptide has comparable affinity to $\alpha v\beta 3$, $\alpha 5\beta 1$ and $\alpha II\beta 3$ at an intermediate level [32] and is useful as no specific integrin is targeted for cell adhesion in our study. Similar to the presentation of the RGD sequence in an exposed loop of a protein [4], the RGD peptide must stand out from an artificial surface in order to reach the binding site of the integrin. With the results presented here (Figure 5) we can conclude that the RGD density grafted on silk is efficient in promoting integrin binding, focal contacts and actin stress fibers formation. The focal adhesion complex is composed of a high density of proteins that attach the extracellular portion of the cell to the intracellular cytoskeletal portion. Integrins attached to the ECM and connected indirectly to the actin filaments through protein assemblies of talin-paxillin-vinculin. These protein assemblies stabilize the focal adhesion structure, as well as relay signals from the ECM to the nucleus. As shown in Figure 5, cells adhering on the multi-grafted silk-functionalized titanium discs present focal contact points, located at the edge of cells. The strong expression of vinculin emphasizes the RGD-Integrin recognition in Swiss3T3 cells grown on multi-grafted silk-functionalized titanium.

Endothelialization testing

Therapeutic success in implantation can be highly dependent on an appropriate colonization of the material by endothelial cells. In this context, we conducted the culture of endothelial side of chick explants on both unmodified and TiBP and RGD-grafted silk -modified titanium. The experiments were carried out after 7 days of culture and showed continuous tissue layers around the explant for both titanium surface compositions (Figure 6). However SEM showed that cells growing on functionalized titanium formed a denser layer compared to the control samples (Figure 6C and F). Migration area and cell density were also the same for explants growing on both control and silk-grafted titanium (Figure 7A and B). To assess endothelial cell adhesion, detachment of the cells was monitored with 10min of diluted-trypsin action. The enzymatic treatment, led to 40% of cells detachment on control titanium whereas only 17% ($p < 0.001$) of cells adhering on multi-grafted silk-coated titanium were detached (Figure 7C) under the same time frame. As a result, we observed stronger endothelial cell adhesion on the titanium functionalized with Silk-TiBP/RGD 5.3%, suggesting better anchoring of the cells. This result is in accordance with the immunolabelling of focal contact points on fibroblasts adhering on grafted-silk coated titanium. Furthermore, this increase in adhesion strength highlight the significance of grafting both Titanium-binding and RGD peptide, as an increase in detachment strength provided with RGD-modified materials is not obvious [6,33].

All together these results reinforce the idea that multi-grafted silk represents a promising tool to modify the surface of implantable medical devices, not only to improve tissue attachment to anchor an implant to surrounding soft tissues but also for complex applications such as blood vessel stenting, when the reendothelialization of the inner part of the stent is needed [34].

Conclusions

We have successfully functionalized silk fibroin protein both with titanium binding peptide (TiBP) and the integrin-binding peptide RGD. This multifunctionalization resulted in increased silk binding to titanium and consequently in improved fibroblast adhesion and proliferation on silk-coated titanium, supporting that RGD density and conformation grafted on silk fibroin is efficient in promoting integrin binding. The bioengineering potential of this modified silk fibroin is reinforced with the results of cultures of endothelium of chick explants showing a strengthened adhesion force. Indeed, coating of a metal biomaterial by endothelial cells is often necessary for success in material implantation. The results presented here could be of major interest for cardiovascular devices such as metallic stents.

Supplementary Material

Refer to Web version on PubMed Central for supplementary material.

Acknowledgments

We thank the European Union for co-funding of equipment within the CPER 2007–2013. We thank Rajesh Naik, AFOSR, for the titanium-binding peptide sequence and Kader Bamouni, Fanny Chapelin and Audrey Jousse for technical assistance. We thank the NIH (P41 EB002520-05 - Tissue Engineering Resource Center) (DLK) for support of this work.

References

- Ikada Y. Surface modification of polymers for medical applications. *Biomaterials*. 1994; 15(10): 725–36. [PubMed: 7986935]
- Rønold HJ, Lyngstadaas SP, Ellingsen JE. A study on the effect of dual blasting with TiO₂ on titanium implant surfaces on functional attachment in bone. *J Biomed Mater Res A*. 2003; 67(2): 524–30. [PubMed: 14566794]
- Variola F, Yi JH, Richert L, Wuest JD, Rosei F, Nanci A. Tailoring the surface properties of Ti6Al4V by controlled chemical oxidation. *Biomaterials*. 2008; 29(10):1285–98. [PubMed: 18155762]
- Pierschbacher MD, Ruoslahti E. Cell attachment activity of fibronectin can be duplicated by small synthetic fragments of the molecule. *Nature*. 1984 May 3–9; 309(5963):30–3. [PubMed: 6325925]
- Massia SP, Stark J. Immobilized RGD peptides on surface-grafted dextran promote biospecific cell attachment. *J Biomed Mater Res*. 2001 Sep 5; 56(3):390–9. [PubMed: 11372057]
- Hersel U, Dahmen C, Kessler H. RGD modified polymers: biomaterials for stimulated cell adhesion and beyond. *Biomaterials*. 2003 Nov; 24(24):4385–415. [PubMed: 12922151]
- Yang C, Cheng K, Weng W, Yang C. Immobilization of RGD peptide on HA coating through a chemical bonding approach. *J Mater Sci: Mater Med*. 2009; 20:2349–2352. [PubMed: 19521750]
- Kasemo B, Gold J. Implant surfaces and interface processes. *Adv Dent Res*. 1999; 13:8–20. [PubMed: 11276751]
- Puleo DA, Nanci A. Understanding and controlling the bone-implant interface. *Biomaterials*. 1999; 20(23–24):2311–21. [PubMed: 10614937]
- Do Serro AP, Fernandes AC, de Jesus Vieira Saramago B. Calcium phosphate deposition on titanium surfaces in the presence of fibronectin. *J Biomed Mater Res*. 2000 Mar 5; 49(3):345–52. [PubMed: 10602067]

11. Oliva FY, Avalor LB, Cámara OR, De Pauli CP. Adsorption of human serum albumin (HSA) onto colloidal TiO₂ particles, Part I. *J Colloid Interface Sci.* 2003 May 15; 261(2):299–311. [PubMed: 16256535]
12. Kriplani K, Kay BK. Selecting peptides for use in nanoscale materials using phage displayed combinatorial peptide libraries. *Curr Opin Biotechnol.* 2005; 16:470–475. [PubMed: 16019201]
13. Baneyx F, Schwartz DT. Selection and analysis of solid-binding peptides. *Curr Opin Biotechnol.* 2007 Aug; 18(4):312–7. [PubMed: 17616387]
14. Sano K, Shiba K. A hexapeptide motif that electrostatically binds to the surface of titanium. *J Am Chem Soc.* 2003 Nov 26; 125(47):14234–5. [PubMed: 14624545]
15. Dickerson MB, Jones SE, Cai Y, Ahmad G, Naik RR, Kröger N, Sandhage KH. Identification and Design of Peptides for the Rapid, High-Yield Formation of Nanoparticulate TiO₂ from Aqueous Solutions at Room Temperature. *Chem Mater.* 2008; 20:1578–1584.
16. Altman GH, Diaz F, Jakuba C, Calabro T, Horan RL, Chen J, Lu H, Richmond J, Kaplan DL. Silk-based biomaterials. *Biomaterials.* 2003 Feb; 24(3):401–16. [PubMed: 12423595]
17. Panilaitis B, Altman GH, Chen J, Jin HJ, Karageorgiou V, Kaplan DL. Macrophage responses to silk. *Biomaterials.* 2003 Aug; 24(18):3079–85. [PubMed: 12895580]
18. Meinel L, Hofmann S, Karageorgiou V, Kirker-Head C, McCool J, Gronowicz G, Zichner L, Langer R, Vunjak-Novakovic G, Kaplan DL. The inflammatory responses to silk films in vitro and in vivo. *Biomaterials.* 2005 Jan; 26(2):147–55. [PubMed: 15207461]
19. Rockwood DN, Preda RC, Yücel T, Wang X, Lovett ML, Kaplan DL. Materials fabrication from *Bombyx mori* silk fibroin. *Nat Protoc.* 2011 Sep 22; 6(10):1612–31. [PubMed: 21959241]
20. Murphy AR, St John P, Kaplan DL. Modification of silk fibroin using diazonium coupling chemistry and the effects on hMSC proliferation and differentiation. *Biomaterials.* 2008 Jul; 29(19):2829–38. [PubMed: 18417206]
21. Vockenroth IK, Rossi C, Shah MR, Köper I. Formation of tethered bilayer lipid membranes probed by various surface sensitive techniques. *Biointerphases.* 2009 Jun; 4(2):19–26. [PubMed: 20408719]
22. Rajaraman R, Rounds DE, Yen SP, Rembaum A. A scanning electron microscope study of cell adhesion and spreading in vitro. *Exp Cell Res.* 1974 Oct; 88(2):327–39. [PubMed: 4426334]
23. Duval JL, Gillissen M, Billy D, Nagel M-D. Use of the Organotypic Culture Method to investigate drug-loaded CSF Shunt. *Journal of Controlled Release.* 2006; 116(2):e50–53. [PubMed: 17718967]
24. Delvat E, Gordin DM, Gloriant T, Duval JL, Nagel M-D. Microstructure, mechanical properties and cytocompatibility of stable beta Ti-Mo-Ta sintered alloys. *Journal of the Mechanical Behavior of Biomedical Materials.* 2008; 1(4):345–351. [PubMed: 19627799]
25. Becker B, Cooper M. A survey of the 2006–2009 quartz crystal microbalance biosensor literature. *Journal of Molecular Recognition.* 2011; 24(5):754–787. [PubMed: 21812051]
26. Höök F, Kasemo B, Nylander T, Fant C, Sott K, Elwing H. Variations in coupled water, viscoelastic properties, and film thickness of a Mefp-1 protein film during adsorption and cross-linking: a quartz crystal microbalance with dissipation monitoring, ellipsometry, and surface plasmon resonance study. *Anal Chem.* 2001 Dec; 73(24):5796–804. [PubMed: 11791547]
27. Chen H, Su X, Neoh KG, Choe WS. QCM-D analysis of binding mechanism of phage particles displaying a constrained heptapeptide with specific affinity to SiO₂ and TiO₂. *Anal Chem.* 2006 Jul 15; 78(14):4872–9. [PubMed: 16841905]
28. Sano K, Sasaki H, Shiba K. Specificity and biomineralization activities of Ti-binding peptide-1 (TBP-1). *Langmuir.* 2005 Mar 29; 21(7):3090–5. [PubMed: 15779989]
29. Chen H, Su X, Neoh KG, Choe WS. Context-dependent adsorption behavior of cyclic and linear peptides on metal oxide surfaces. *Langmuir.* 2009; 25(3):1588–93. [PubMed: 19170646]
30. Baino F, Vitale-Brovarone C. Three-dimensional glass-derived scaffolds for bone tissue engineering: current trends and forecasts for the future. *J Biomed Mater Res A.* 2011 Jun 15; 97(4):514–35. [PubMed: 21465645]
31. Ziegler WH, Liddington RC, Critchley DR. The structure and regulation of vinculin. *Trends Cell Biol.* 2006 Sep; 16(9):453–60. [PubMed: 16893648]

32. Ruoslahti E, Pierschbacher MD. New perspectives in cell adhesion: RGD and integrins. *Science*. 1987; 238(4826):491–7. [PubMed: 2821619]
33. Rezaia A, Carson HT, Branger AB, Waters CM, Healy KE. The detachment strength and morphology of bone cells contacting materials modified with a peptide sequence found within bone sialoprotein. *Journal of Biomedical Materials Research*. 1996 Oct; 37(1):9–19. [PubMed: 9335344]
34. de Mel A, Jell G, Stevens MM, Seifalian AM. Biofunctionalization of biomaterials for accelerated in situ endothelialization: a review. *Biomacromolecules*. 2008; 9(11):2969–79. [PubMed: 18831592]

\$watermark-text

\$watermark-text

\$watermark-text

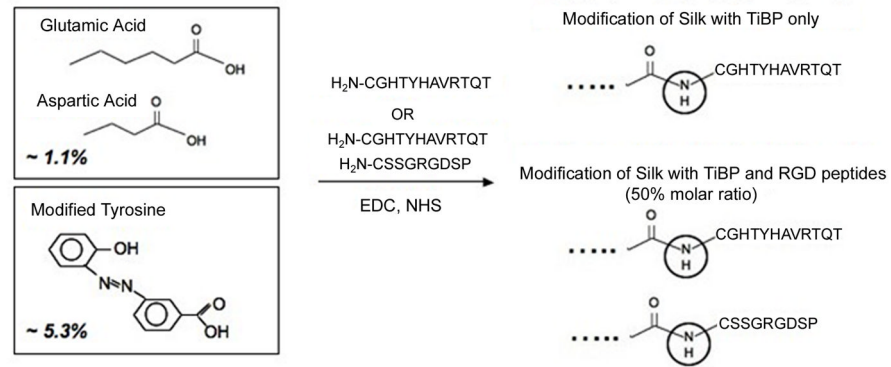


Figure 1. Chemical modification of Silk Fibroin with titanium-binding (TiBP) and RGD peptides

Two methods were used to graft the silk with peptides:

1- Carbodiimide coupling: silk fibroin contains a significant number of aspartic acid (0.5 mol%) and glutamic acid (0.6 mol%). Coupling reactions of the amine group of either TiBP and RGD was carried out with the carboxylic acid group of aspartic and glutamic acids of the soluble silk protein in aqueous solutions through carbodiimide coupling, resulting in 1.1 mol% modified silk fibroin. **2- Diazonium coupling:** silk fibroin contains also 5.3 mol% of tyrosine. Methods to functionalize silk fibroin using diazonium coupling chemistry resulted in a 6.4 mol% modified silk fibroin.

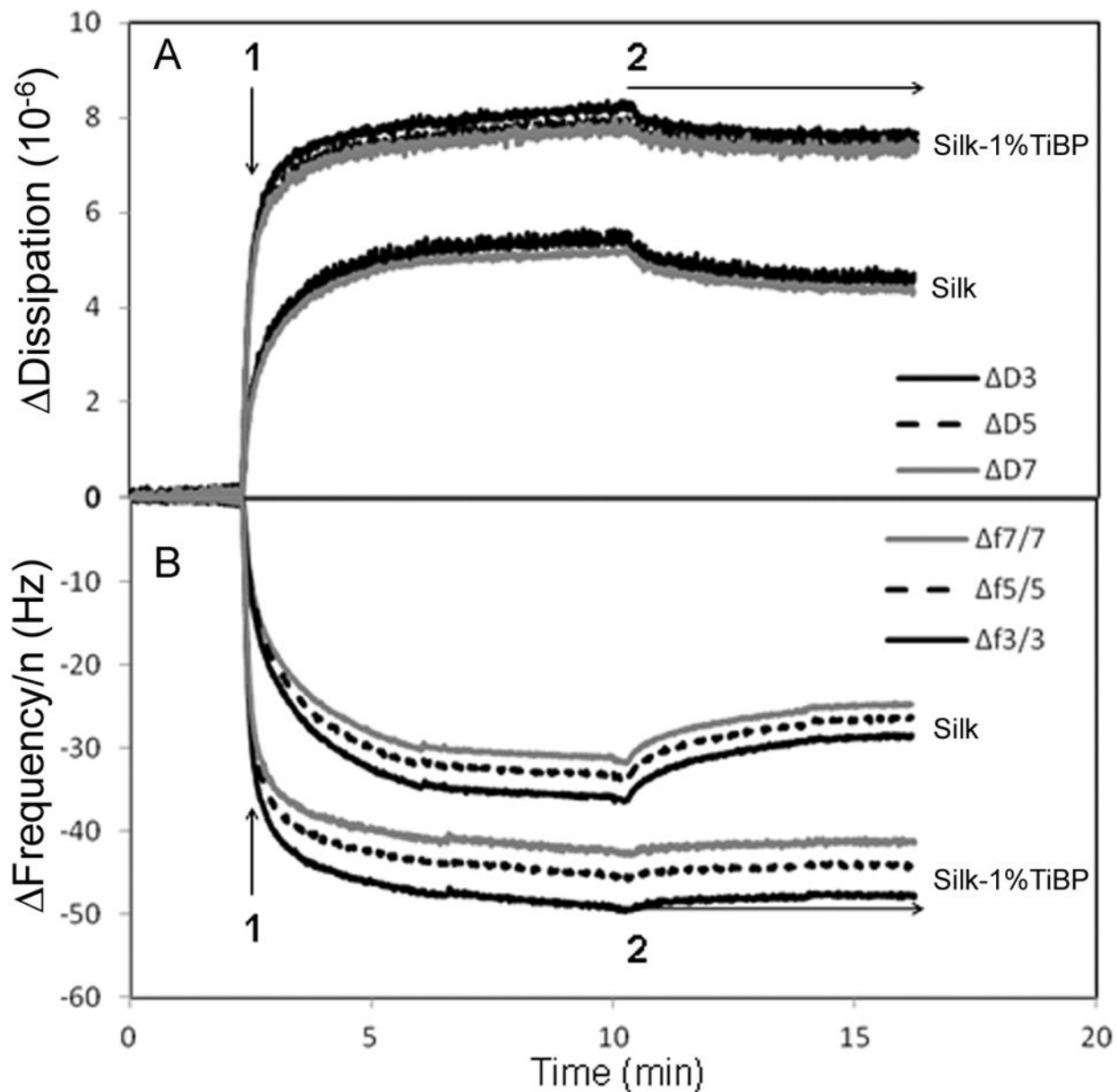


Figure 2. QCM-D analyses of the unmodified and the 1% TiBP functionalized silk protein binding to a titanium coated quartz crystal

Binding of unmodified silk and binding of 1% TiBP-silk protein on TiO_2 coated quartz crystals, detected by dissipation (ΔD_n , panel A) and frequency (Δf_n , panel B) shifts at three overtones, $n=3$ (15 MHz), $n=5$ (25 MHz) and $n=7$ (35 MHz). Arrow 1: Protein injection; Arrow 2: buffer rinsing.

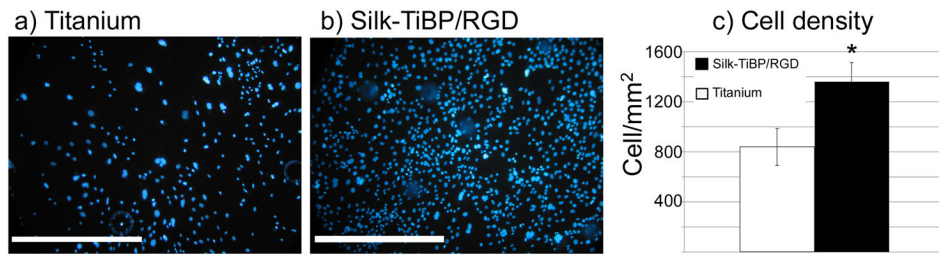


Figure 3. Influence of titanium-coating on adherent cell density
Fluorescence micrographs of DAPI-stained nuclei of fibroblasts grown for 48h on a) control titanium, b) titanium+Silk-TiBP/RGD 5.3%, c) Average cell density adhering 48h after seeding (*p<0.01). Scale bar: 500 μ m.

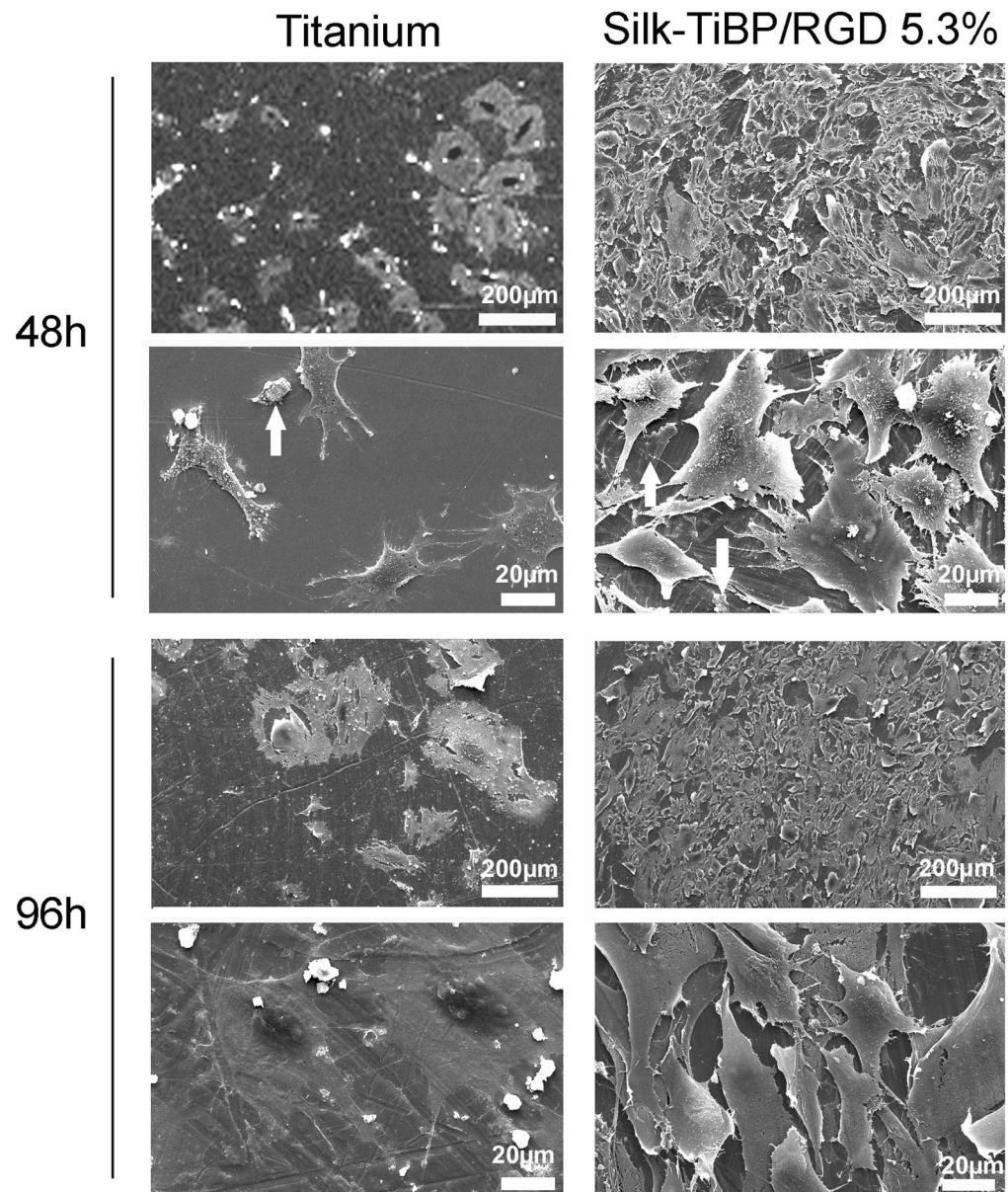


Figure 4. SEM images of cell adhering and spreading on titanium discs
SEM micrographs of the attachment and spreading of fibroblasts on titanium discs and titanium functionalized with Silk-TiBP/RGD 5.3% after 48 and 96h.

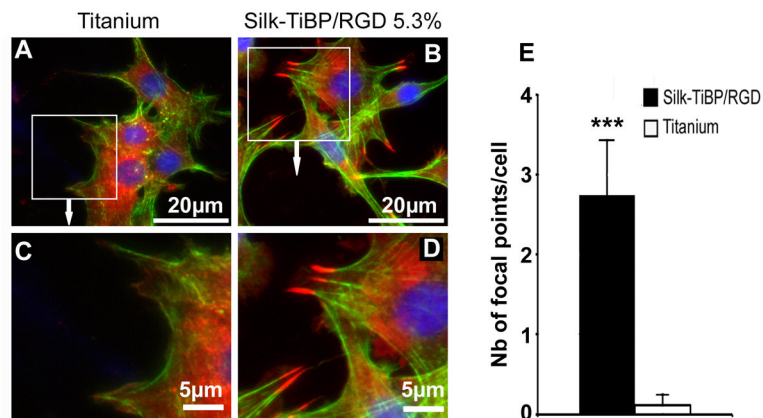


Figure 5. Fluorescence microscopy images of adherent cells on titanium discs and focal contact points' quantification

Immunolocalization of vinculin (red), actin (green) and nuclei (blue) in Swiss 3T3 cells grown for 4h on uncoated titanium control (A, C) and Silk-TiBP/RGD 5.3% (B,D). Cell spreading is evidenced by the actin staining in green. Vinculin staining was observed as dots with punctuate distribution around the membrane periphery for cells grown on Silk-TiBP/RGD 5.3%. Dots are localized at the end of actin fibers to form focal contacts (B and D). Focal contact points' quantification (E) was realized as described in material and methods. Results were compared using a Mann–Whitney test with $p < 0.001$ (***)

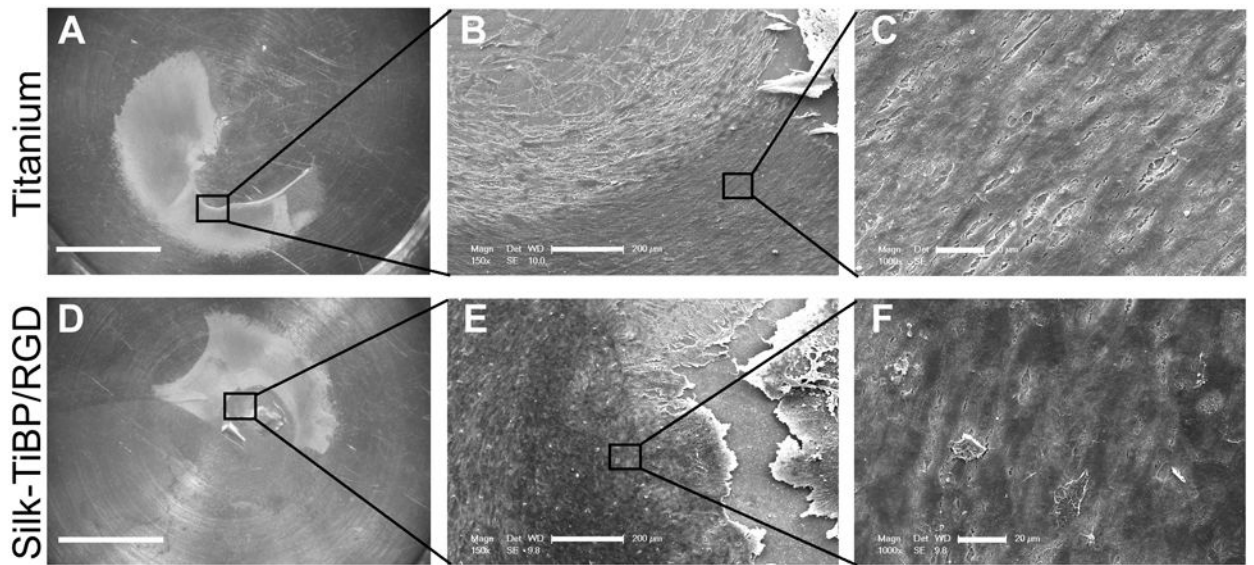


Figure 6. Endothelial tissue culture

Organotypic tissue culture was realized on unmodified titanium discs (a, b, c) or functionalized with silk-TiBP/RGD 5.3% (d,e,f). Images a and d show the tissue expanding on titanium surface. SEM micrographs of explant at low magnification (b,e) and higher magnification (c,f) reveal the growing cells layer. Scale bars: a,d: 5mm; b,e: 200μm; c,f: 20μm.

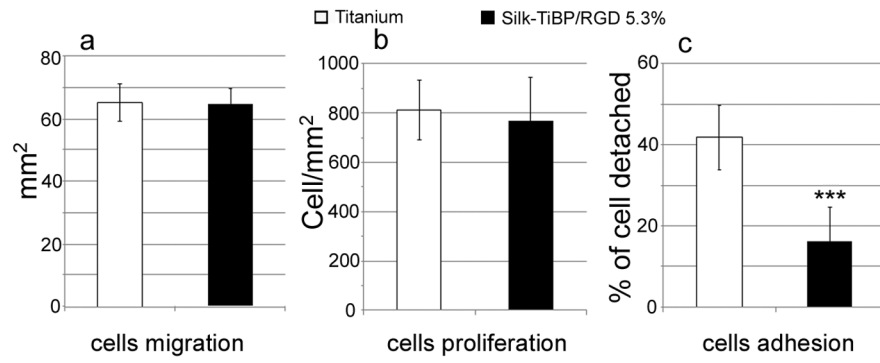


Figure 7. Endothelial cells migration, proliferation and adhesion

Cytocompatibility of titanium (white) and titanium+Silk-TiBP/RGD 5.3% (black) as a function of cellular migration (a), proliferation (b) and adhesion (c). Titanium n=12, titanium+Silk-TiBP/RGD 5.3%, n=16. *** p< 0.001. Kruskal–Wallis one-way analysis of variance test.

Table 1

Degree of substitution of the Silk-diazo derivatives modified with RGD and or Ti-BP as calculated by the AA composition analysis:

sample	DS in RGD (mol %)	DS in Ti-BP (mol %)
Silk-RGD 5.3%	4.8 % ^a	-
Silk-TiBP 5.3%	-	2.2 ^b – 2.7 % ^c
Silk-TiBP/RGD 5.3%	1.4 % ^a	1.6 ^b – 2.0 ^c %

^a based on the increase of Arg

^b based on the increase of Thr

^c based on the increase of Hys